ELSEVIER

Polymer 42 (2001) 801–806

polymer

www.elsevier.nl/locate/polymer

Phase behavior, photopolymerization, and morphology development in mixtures of eutectic nematic liquid crystal and photocurable monomer

D. Nwabunma, T. Kyu*

Institute of Polymer Engineering, The University of Akron, Akron, OH 44325-0301, USA

Received 20 December 1999; received in revised form 3 May 2000; accepted 3 May 2000

Abstract

Phase behavior and photopolymerization-induced morphology development in mixtures of eutectic nematic liquid crystals (LC) (designated E44) and photocurative monomers (designated NOA65) have been investigated by means of optical microscopy and light scattering. The observed phase diagram of the E44/NOA65 system prior to photopolymerization is of an upper critical solution temperature (UCST) type overlapping with the nematic–isotropic transition of E44. It displayed isotropic liquid, isotropic liquid + isotropic liquid, isotropic liquid + nematic, and pure nematic coexistence regions that were verified experimentally. Using the phase diagram as a guide, photopolymerization-induced phase separation experiments were performed in the isotropic region in order to examine the morphology development in multicomponent LC (E44)-based system in comparison with that of a single component LC (K21)-based system. Of particular interest is that the emerging LC droplets turned out to be unevenly distributed in the E44/NOA65 system as opposed to the K21/NOA65 system where the droplet size was uniform. The non-uniform distribution of the droplets in the E44/NOA65 system may be attributed to compositional fractionation associated with different affinities of the constituent LC in E44 to the NOA65 networks.

Keywords: Phase diagram; Photopolymerization-induced phase separation; Morphology development

1. Introduction

Inhomogeneous thin films composed of liquid crystals (LC) and polymers have been investigated extensively for applications in various electro-optical control and display devices such as optical shutters, switchable privacy windows, and reflective color displays [1,2]. These investigations encompass synthesis of new materials, phase behavior, morphological characterization, polymerization kinetics, phase separation dynamics, electro-optical characterization, and optimization of device performance [3–9]. LC/polymer composites are normally prepared via polymerization-induced phase separation (PIPS) of an initially miscible solution of LC and polymer precursor. The phase separation process turns out to be one of the most important steps for controlling LC domain morphology and efficient fabrication of these films.

In previous papers [10,11], we have investigated the phase behavior, polymerization kinetics, and emergence of morphology in mixtures of the single component nematic LC 4-*n*-heptyl-4′-cyanobiphenyl (commercially known as K21) and photocurable polymer precursor (NOA65). It was shown that the morphology development in the K21/NOA65 system was influenced strongly by photopolymerization environment (e.g. single or two-phase coexistence regions) as well as polymerization conditions such as irradiation time, temperature, etc. K21, being a single component LC, is appealing for basic studies involving establishment of phase diagram and elucidation of phase separation dynamics in its blends with photocurative materials. However, it is unsuitable for practical applications due to a very small nematic window bound by the nematic–isotropic transition temperature ($T_{NI} = 42°C$) and the crystal–nematic transition temperature ($T_{KN} = 28.5°C$). To widen the nematic temperature range for electro-optical applications, it is customary to mix two or more LC moieties [7–9]. Eutectic LC mixtures with wide nematic temperature range are thus preferred to the single component LC in industrial applications. Hence, understanding photopolymerization-induced morphology development in multicomponent LC/photocurative systems is of paramount interest.

In this paper, we have extended our investigations to a system composed of eutectic nematic LC (E44) and NOA65. The aim is to examine the influence of LC type (single component K21 versus multi-component eutectic

* Corresponding author. Tel.: +1-330-972-6865; fax: +1-330-258-2339.
E-mail address: tkyu@uakron.edu (T. Kyu).

0032-3861/01/$ - see front matter
PII: S0032-3861(00)00368-2

E44) on the morphology development in LC/polymer composites prepared via photopolymerization-induced phase separation. The choice of E44 is two-fold. First it is a eutectic mixture having a very wide nematic region, which makes it suitable for use in polymer-dispersed liquid crystal (PDLC) based electro-optical switches and windows. Second, the nematic–isotropic temperature T_{NI} is very high ($T_{NI} = 108°C$) relative to other eutectic mixture such as E7 (61°C) [12]. In this paper, we first establish the phase diagram of the E44/uncured NOA65 followed by kinetics of photopolymerization. Using the phase diagram as a guide, the photopolymerization-driven morphology development in the E44/NOA65 system is examined in comparison with that of the K21/NOA65 system. Of particular interest is that the emerging LC droplets in the E44/NOA65 system showed bimodal droplet sizes with uneven distribution as opposed to the K21/NOA65 system where droplet distribution was uniform. A possible cause for the non-uniformity of LC droplet size and distribution in the E44/NOA65 system is suggested.

2. Experimental

2.1. Material and preparation of mixtures

A eutectic nematic LC (E44) having $T_{KN} = 6°C$ and $T_{NI} = 108°C$ and a single component nematic LC, 4-*n*-heptyl-4′-cyanobiphenyl (K21) having $T_{KI} = 28.5°C$ and $T_{NI} = 42°C$, were purchased from BDH Chemicals. Photocurable precursor (NOA65) was purchased from Norland Products Inc. NOA65, consisting of trimethylol-propane diallyl ether, trimethylol-propane tris thiol, and isophorone diisocyanate ester, is reported to be premixed with 5 wt% benzophenone photoinitiator [14,15]. NOA65 has a maximum absorption in the 350–380 nm wavelength and the weight average molecular weight of 400 g/mol.

2.2. Establishment of E44/uncured NOA65 phase diagram

E44/NOA65 mixtures were prepared by weighing appropriate amounts of NOA65 and E44 in small vials, which were then mixed thoroughly. The samples were stored in a refrigerator and handled under dimmed room light to prevent any unwarranted prepolymerization. For the optical microscopy experiment, a Nikon Optipot 2-POL microscope with a filtered Halogen light source (12 V, 100 W) was used. Pictures were taken using a Nikon FX-35DX camera connected to a Nikon UFX-DX exposure controller. A sample hot-stage (Model TS1500, Linkam Scientific Instruments) interlinked with a programmable temperature controller (Model TMS93) and a cooling unit (Model LNP93/2) was used. Samples were heated until optically clear and any phase change was observed under the microscope during slow cooling. Thereafter, the samples were reheated to the isotropic state. The heating and cooling rate was 1°C/min. Since the phase transition is thermally reversible, the phase transition temperatures may be determined by repeating the heating and cooling cycles in a small temperature gap near the phase transition temperatures.

For light scattering experiments, a 2 mW randomly polarized He–Ne laser light source (Aerotech, Model LSR2R) with a wavelength of 632.8 nm was utilized. Cloud points were measured by monitoring the scattered intensity at a fixed angle (~10°) using a photodiode detector (Hamamatsu Co., Model HC-220-01). A sample hot stage coupled with a programmable temperature controller (Omega, Model CN-2012) was utilized for temperature scans at the rate of 1°C/min. A personal computer and an A/D converter were linked to the light scattering equipment for data acquisition.

2.3. Photopolymerization cure kinetics

Photopolymerization of various E44/NOA65 mixtures having 70–95% LC was monitored at an isothermal temperature of 60°C using a Perkin–Elmer photo-DSC instrument equipped with a dual beam photo-calorimetric accessory (DSC-DPA7) including a xenon light source (450 W) and a monochromator to select UV radiation of a specific wavelength (366 nm). Mixtures prepared as described above were weighed in the recommended amount (~10 mg) into hermetic aluminum DSC pans. Prior to exposing samples to UV radiation, the DSC cell was flushed with nitrogen for about 5 min to prevent oxidation. Samples were heated to the isotropic region to ensure homogeneity in film thickness and to afford the same thermal history. Subsequently, they were brought back to the intended experimental temperatures. The samples and the reference pans were left open during photopolymerization. The heat flow versus time data from the photo-DSC was used to calculate the experimental conversion rate and the photopolymerization rate according to the procedure reported earlier [10]. Since LC is not directly involved in the photoreaction, the heat flow curved was normalized based on the NOA65 content. For details, interested readers are referred to the earlier paper [10].

2.4. Preparation of E44/crosslinked NOA65 composites

For the fabrication of E44/crosslinked NOA65 composites, various starting mixtures were placed on microscope glass slides covered with circular cover glasses for thickness uniformity. These samples yielding a thickness range of 10–20 μm were photopolymerized under the optical microscope. The photo-crosslinking was performed on the optical microscope at 60°C using an UV curing unit (Model ELC403, Electrolite Corporation). The instrument output was 40 mW/cm^2 in the 350–380 nm wavelength range.

The curing unit allowed for both continuous and intermittent irradiation. Samples of small area were used to ensure uniform radiation and to minimize the effect of thickness on the absorbed radiation and the emerging structures. The irradiation intensity was maintained at 40 mW for all

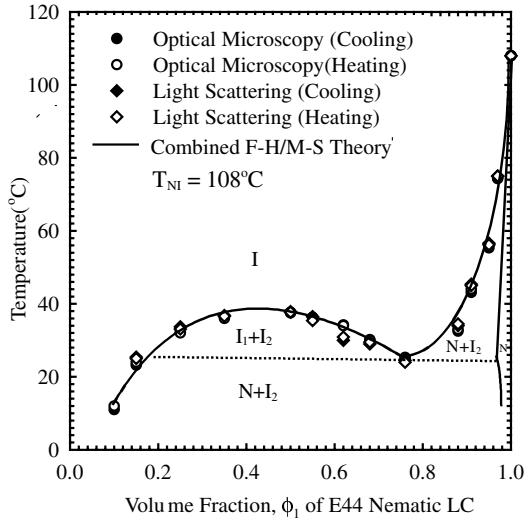

Fig. 1. Phase diagram of uncured mixtures of E44 and NOA65 as obtained using optical microscopy and light scattering. The solid line denotes the theoretical curve calculated based on the combined theories of Flory–Huggins and Maier–Saupe (FH/MS).

samples having an average area of 1 cm^2. The microscopic pictures showing the emerging morphology were then examined as a function LC concentration and irradiation time.

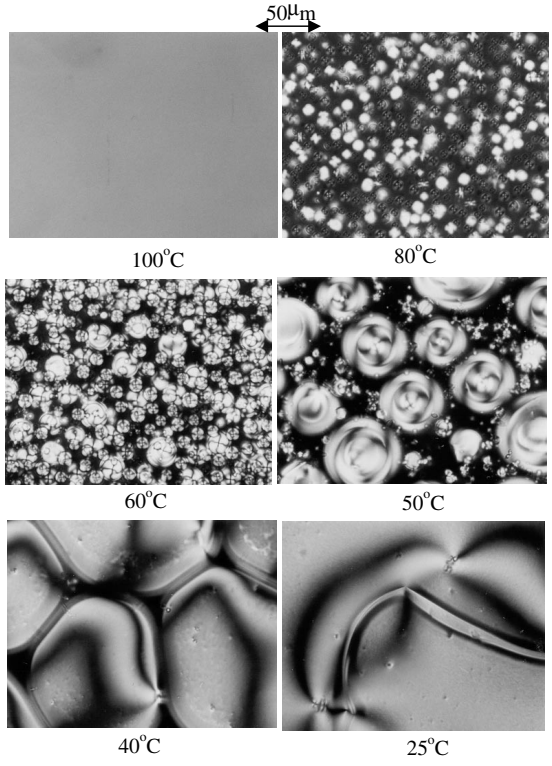

Fig. 2. Morphological pictures showing isotropic liquid (100°C) and liquid + nematic (80, 60, 50, 40, and 25°C) coexistence regions observed during cooling of uncured 95/05 E44/NOA65 mixture. Cooling rate was 1°C/min.

3. Results and discussion

3.1. Phase diagram of E44/uncured NOA65

Fig. 1 shows the observed phase diagram in comparison with the theoretical curve (solid line). The theoretical phase diagram of nematic LC/flexible monomer mixture was calculated based on the combined Flory–Huggins/Maier–Saupe (FH/MS) theory [16–23]. The phase diagram is typically of a UCST type intersecting with the nematic–isotropic transition of E44 [16]. The LC/monomer phase diagram shows strong resemblance to those reported for other mixtures of nematic LC and flexible monomer or with linear polymer [10,16,23,25,26], except that the UCST is asymmetric in the latter case of the LC/linear polymer.

The phase diagram reveals isotropic (I), isotropic liquid + isotropic liquid ($I_1 + I_2$), isotropic liquid + nematic (I_2 + N), and pure nematic (N) coexistence regions. At the peritectic point (delineated by dotted horizontal line) these three phases can coexist. These regions were further identified experimentally by monitoring the emergence of LC domains under the optical microscope. Upon cooling the 95/05 mixture from an isotropic phase (100°C) to a two-phase region (around 84°C), multiple birefringent droplets appear as a dispersed phase in the continuum of dark background suggestive of the isotropic liquid + nematic (I_2 + N) coexistence region (Fig. 2). With subsequent cooling, these birefringent droplets grow via coalescence (60 and 50°C), while exhibiting complex topologies of LC disclinations. The smaller domains are seemingly annihilated as the larger ones continue to grow at the expense of the smaller ones. The textures emerge into bipolar droplets at 40°C and finally the domain boundaries disappear at 25°C resulting in a typical Schlieren texture.

3.2. Photopolymerization behavior

Fig. 3a shows the experimental conversion rate as a function of time for three E44/NOA65 mixtures. Note that these mixtures were initially in the isotropic phase at 60°C before photopolymerization. In the neat NOA65, the conversion arises instantaneously without any induction time, suggesting rapid generation of polymer radicals for chain propagation (Fig. 3b). The conversion eventually reaches a limiting value, implying that a full conversion may be not realized because of the diffusion-limited propagation caused by network formation. The conversion rate quickly reaches a maximum value within a few seconds as the chain propagation occurs. When the termination reaction becomes dominant over the propagation, the conversion rate decays rapidly and approaches zero asymptotically with time due to reduced polymer radical mobility, monomer depletion, and termination. As the initial monomer (NOA65) concentration in the mixtures is reduced, the maximum conversion rate decreases, and likewise the limiting value of the conversion. This behavior is expected because LC molecules,

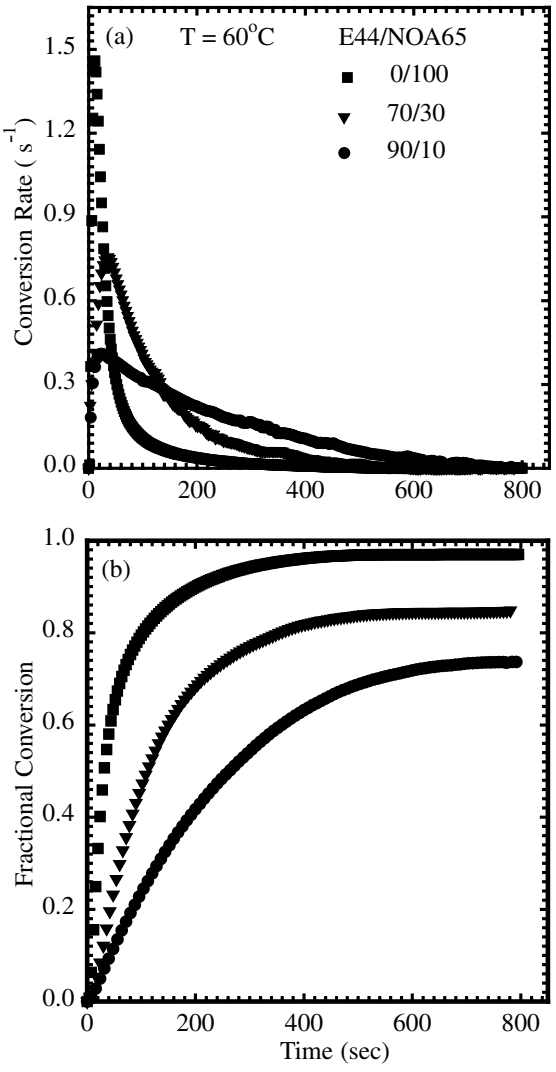

Fig. 3. Variation of experimental conversion rate and fractional conversion with time for 0/100, 70/30, and 90/10 E44/NOA65 mixture photopolymerized in the isotropic phase at 60°C.

which are not directly involved in the reaction, must segregate out from the emerging network. It is interesting to point out that we have observed the same behavior previously in the UV-curing of the K21/NOA65 system [10]. Guymon and Bowman [5,24] also reported a similar rate behavior for UV-cured smectic C*/acrylate and smectic C*/diacrylate systems, except that they found additional rate enhancement, which has been attributed to monomer segregation in the smectic C* layers.

3.3. Morphology development

It has been demonstrated that polymerization initiated in the two-phase region of the LC/monomer phase diagram results in non-uniform droplet morphology [10,13], which is undesirable for electro-optical applications. The major problem associated with PIPS in the two-phase region is due to pre-existing structures. As demonstrated in Fig. 3a,

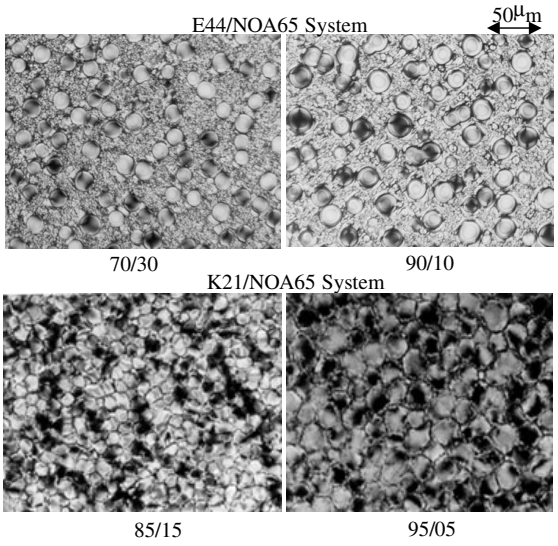

Fig. 4. Morphologies of the 70/30 and 90/10 E44/NOA65 mixtures photopolymerized in the isotropic phase at 60°C in comparison with those of the 85/15 and 95/05 K21/NOA65 mixtures photopolymerized at 40°C. UV intensity was 40 mW/cm^2 and irradiation time was 5 min.

the conversion rate depends on the local concentration of NOA65, hence any heterogeneity in concentration would lead to the non-uniform morphology resulting in the formation of large and small LC droplets. To circumvent the aforementioned problem, we shall focus only on photopolymerization initiated in the isotropic state where the initial concentration is uniform everywhere.

Fig. 4 shows the morphology of two E44/cured NOA65 compositions in comparison with two other compositions of the K21/cured NOA65 system. Both systems were subjected to the same UV-intensity level and exposure time, except that the K21/NOA mixture was cured in the isotropic region at 40°C (see Ref. [10]; Fig. 1) as opposed to the E44/NOA65 system that was cured in the isotropic region at 60°C (Fig. 1). It should be noted that the unification to either temperature becomes impractical because the 90/10 or 95/5 E44/NOA65 mixtures would be in the two-phase at 40°C, whereas the corresponding K21/NOA65 blends would be in the isotropic state at 60°C even after curing. These two separate temperatures were chosen so that the mixtures are in the isotropic region before polymerization, but in the two-phase isotropic + nematic region after photopolymerization.

Fig. 4 shows the comparison of domain morphologies for the photochemically cured E44/NOA65 and K21/NOA65 blends at two different compositions. In thermal-quench systems, the average domain size simply depends on the supercooling. However, the size dependence on concentration in a polymerizing system is more complex as the UCST coexistence curve moves up asymmetrically with increasing molecular weight of the reacting component. The phase diagram of the LC/crosslinked polymer system is skewed without exhibiting a critical point [11]. Moreover, the

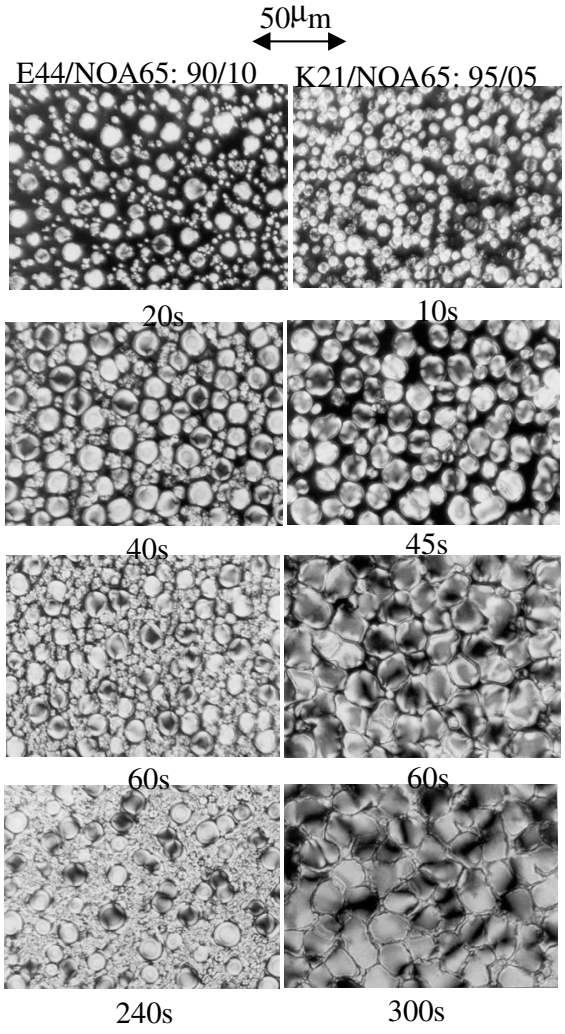

Fig. 5. Time evolution of morphology during photopolymerization of the 90/10 E44/NOA65 mixture in the isotropic phase in comparison with that of the 95/05 K21/NOA65 mixture. Samples were irradiated up to the indicated times, and then the UV light quickly turned off before taking pictures. UV intensity was 40 mW/cm^2.

coexistence curve near the pure LC axis shows a drastic increase, thus the supercooling, i.e. the difference in the reaction temperature and the coexistence point of the LC/polymer network, would be very sensitive to the LC concentration. Another scenario is that the photopolymerization rate, as evidenced in Fig. 3, is slower at higher LC concentrations, thereby allowing more time for LC molecules to segregate out which in turn leads to larger domains.

Although both systems exhibit LC droplet morphology, there are some notable differences in Fig. 4. It is apparent that the LC droplets in the E44/NOA65 mixtures are bimodal consisting of large and small domains. The primary LC domain texture in the larger droplets is of a bipolar type. In the K21/NOA65 mixtures, the droplet size is more or less uniform with polygonal topology. The polygonal texture may be ascribed to the impingement effect of the neighboring domains. This observation is consistent with the earlier works of Amundson et al. [4], Serbutoviez et al. [27] and Carter et al. [28] who found similar morphologies in LC/photocured diacrylate systems.

The observed uniform morphology in the K21/cured NOA65 system is therefore not surprising in view of the fact that K21 is a single component LC. On the other hand, E44 is a mixture of several LC, thus fractionation into components could occur during photopolymerization. The LC moieties present in E44 phase separate presumably at different rates from the cured NOA65 matrix. That is to say the individual LC moieties may have different affinities to NOA65, therefore separating out at different rates. Another possibility is that the as-received E44 may not be strictly eutectic; any slight deviation from the azeotropic point in the E44 mixture could result in phase separation among the constituent LC. Since photopolymerization is inherently very fast, any non-uniform structures may be pinned down by virtue of the rapid network formation.

Since the growth dynamics is non-linear and non-equilibrium in character, it is of interest to investigate the time evolution of structures during photopolymerization. In a previous paper [13], we have demonstrated that the intermittent illumination approach is useful in probing the dynamics of photopolymerization-induced phase separation by optical microscopy. In this approach, the samples were irradiated for desired times, and then the UV light quickly turned off a few seconds to acquire images and turned on again. This method was employed to circumvent the difficulty of probing the phase separation dynamics in real time using the conventional time-resolved light scattering set-up because of strong interference of the UV intensity with the scattered laser light. It was found that there is little or no difference in the emerging patterns between the intermittent and continuous UV illumination of the K21/NOA65 system.

Fig. 5 depicts the temporal evolution of morphology for the 90/10 E44/NOA65 mixture in comparison with that of the 95/05 K21/NOA65 mixture. The comparison for the emergence of domain morphology in two different compositions is by no means ideal, but it may be justifiable because both mixtures are in the isotropic state before photopolymerization, but in the same I + N coexistence region during and after curing. Upon UV irradiation, phase separation starts almost instantaneously, typical within a few percent conversions [10,13,27] due to the fast nature of photopolymerization. At 20 s, the emerged LC domain are of spherical droplets and appear more or less uniform for the K21/NOA65 system, whereas a bimodal distribution of droplet sizes can be discerned in the E44/NOA65. With continued irradiation, the droplets quickly grow in size via coalescence. When these droplets impede into each other, the droplet morphology transforms into the polygonal shape. The polygonal boundaries are eventually frozen in place with the progression of the crosslinking reaction in which LC molecules are trapped in a matrix of crosslinked NOA65. In the E44/NOA65 system, the droplet morphology simply ceases to grow when the crosslinking reaction

advances. One may conclude that although the E44/NOA65 system may be used as PDLC because of its wide nematic range, it suffers a setback due to the heterogeneity of the droplet sizes. On the other hand, the uniform morphology of the K21/NOA65 system may be appealing, however, the limited nematic region makes the K21-based PDLC impractical.

4. Conclusions

In this work, we have examined the phase behavior, cure kinetics, and morphology development in the UV-cured E44/NOA65 system. The phase diagram of the uncured E44/NOA65 system is of the UCST type overlapping with the nematic isotropic transition of E44. It displayed isotropic liquid, isotropic liquid + isotropic liquid, isotropic liquid + nematic, and pure nematic coexistence regions. Using the phase diagram as a guide, the cure kinetics was examined by means of the photo-DSC technique. It was found that the maximum conversion rate increases with initial NOA65 concentration consistent with the reported results for other systems. Full conversion of monomer is unattainable possibly due to of the diffusion-limited propagation arising from network formation. In regard to morphology development, it was found that the LC droplets showed a bimodal distribution in the cured E44/NOA65 system, but appeared monodispersed with a uniform distribution in the cured K21/NOA65 system. Since E44 is a mixture of several LC, the observed heterogeneity may be due to compositional fractionation, causing the LC moieties in the E44 to segregate at different rates from the cured NOA65 matrix. The time evolution of morphology confirmed that the LC droplet phase separated into non-uniform small droplets in the E44/NOA system. These droplets grew via coalescence until the structures were fixed by network formation.

Acknowledgements

Support of this work by the NSF-STC ALCOM (Advanced Liquid Crystal Optical Material Center) through Grant Number DMR 89-20147 is gratefully acknowledged.

References

[1] Doane JW. In: Bahadur B, editor. Liquid crystal: applications and uses, Singapore: World Scientific, 1990. p. 361.
[2] West J. In: Mckay RB, editor. Technological application of dispersions, New York: Marcel Dekker, 1994. p. 345.
[3] Doane JW, Golemme A, West JL, Whitehead JB, Wu BG. Mol Cryst Liq Cryst 1988;165:511.
[4] Amundson K, van Blaaderen A, Wiltzius P. Phys Rev E 1997; 55:1646.
[5] Guymon CA, Hoggan EN, Walba DM, Clark NA, Bowman CN. Liq Cryst 1995;19:719.
[6] Hikmet RAM. J Appl Phys 1990;68:4406.
[7] Hirai R, Niiyama S, Kumai H, Gunjima T. Proc SPIE-Int Soc Opt Engng 1990;1257:2.
[8] LeGrange JD, Miller TM, Wiltzius P, Amundson KJ, Boo J, van Blaaderen A, Srinivasarao M, Kmetz A. SID Digest 1995;193:275.
[9] Nolan P, Tillin M, Coates D. Mol Cryst Liq Cryst Lett 1992;8:129.
[10] Nwabunma D, Kim KJ, Lin Y, Chen LC, Kyu T. Macromolecules 1998;31:6806.
[11] Nwabunma D, Kyu T. Macromolecules 1999;32:664.
[12] Kajiyama T, Kikuchi H, Takahara A. Liquid crystal materials devices, and applications. SPIE 1992;1665:20.
[13] Nwabunma D, Chiu HW, Kyu T. Macromolecules 2000;33:1416.
[14] Technical Data Sheet for NOA65 Optical Adhesive, Norland Products, Inc., New Brunswick, NJ.
[15] Smith GW. Mol Cryst Liq Cryst 1991;196:89.
[16] Shen C, Kyu TJ. Chem Phys 1995;102:556.
[17] Chiu HW, Kyu TJ. Chem Phys 1995;103:7471.
[18] Flory PJ. J Chem Phys 1942;10:51.
[19] Huggins ML. J Chem Phys 1941;9:440.
[20] Maier W, Saupe A. Naturforsch 1958;A13:564.
[21] Maier W, Saupe A. Naturforsch 1959;A14:882.
[22] Maier W, Saupe A. Naturforsch 1960;A15:287.
[23] Benmouna F, Bedjaoui L, Maschke U, Coqueret X, Benmouna M. Macromol Theory Simulat 1998;7:599.
[24] Guymon CA, Bowman CN. Macromolecules 1997;30:5271.
[25] Kim WK, Kyu T. Mol Cryst Liq Cryst 1994;250:131.
[26] Lin Z, Zhang H, Yang Y. Macromol Chem Phys 1999;200:943.
[27] Serbutoviez C, Kloosterboer JG, Boots HMJ, Touwslager FJ. Macromolecules 1996;29:7690.
[28] Carter SA, LeGrange JD, White W, Boo J, Wiltzius P. J Appl Phys 1997;81:5992.